Green tea mediated synthesis of silver nanoparticles in halloysite nanotubes and their potential antimicrobial properties

K. Sudhakar[1*], S. J. Moloi[1], K. Madhusudana Rao[2]

1. Department of Physics, University of South Africa, Private Bag X6, Florida 1710, South Africa.
2 School of Chemical Engineering, Yeungnam University, 280-Daehak-Ro, Gyeongsan 712-749, South Korea

Abstract

A simple method has been developed for production of silver nanoparticles (Ag-NPs) in the halloysite nanotubes (HNTs) using green tea (GT) as reducing agent in this work. The formation of HNTs/Ag-NPs was confirmed by UV-Visible spectroscopy, scanning electron microscopy, X-ray photoelectron spectrometry and X-ray diffraction pattern. Transmission electron microscopy results revealed that the spherical and homogeneously distributed Ag-NPs are formed in the lumen as well as in the surface silicate cage of HNTs. The obtained HNTs/Ag-NPs showed good antibacterial activity towards *E.coli* and *B.subtilis*. In general, the results indicate that the prepared hybrid silver nanocomposites are low cost materials and can be applied potentially for advanced medical applications.

1. Introduction

Hybrid silver nanoparticles (Ag-NPs) have generated essential interest because of their potential applications in optics, electronics, catalysis, and biomedical applications [1-4]. Expansion of novel Ag-NPs containing products exhibit significant role in the nano technology. In particular, there is an increasing interest towards the exploitation of Ag-NPs technology in the development of bioactive materials, aiming at combining the relevant antibacterial properties of the metal with the peculiar performance of the biomaterials [5-7]. A various combining materials are used for the incorporation of Ag-NPs, such as clay materials, carbon nanotubes, and polymeric materials [8-10]. Among these, the incorporation of Ag-NPs in clay materials are inexpensive and abundant [11]. In specifically, halloysite nanoclay minerals are naturally occurring aluminosilicates with a hollow tubular structure like carbon nanotubes. The length of the halloysite nanotubes (HNTs) is in the range of 0.2-1.5μm, whereas the inner and outer diameters of tubes are 10–30nm and 40–70 nm, respectively [12]. These materials can be produced in huge quantities and highly biocompatible [13]. HNTs are a viable nanocage for the inclusion of biologically-active molecules with specific sizes due to the empty lumen space of the HNTs. HNTs has many potential applications, such as the controlled release of anti-corrosion agents, herbicides and fungicides [14-16].

Recent reports showed that the Ag-NPs were generated in the HNTs using conventional chemical reduction methods [17]. Ag-NPs was prepared in the lumen structure of HNTs by applying thermal heating [18]. However, these methods need more thermal energy and have toxic reducing agents that are harmful for living systems. Consequently, herein we reported a simple method for the preparation of Ag-NPs via *insitu* method in to the HNTs using green tea (GT) as reducing agent. In this process GT was used as a strong and rapid reducing agent for silver nitrate being with colloidally stable of Ag-NPs in the lumen structure as well as silicate cage of HNTs. The obtained HNTs/Ag-NPs hybrid systems are studied using different characterization techniques and applied for antibacterial applications.

2. Materials and Experimental details

2.1. Materials

Halloysite nano clay was purchased from Aldrich chemicals co. U.S.A. and silver nitrate was purchased from Merck Specialities Pvt.Ltd. Mumbai, India. Green tea (80% polyphenols) extract was obtained from Natural

remedies Pvt. Ltd. Bangalore India. Mill-Q water used in this work was obtained from Civil & Chemical engineering of UNISA in South Africa.

2.2. Preparation of HNTs/Ag-NPs hybrid material

For the fabrication of HNTs/GT/Ag-NPs hybrid material, 0.5 g HNTs was dispersed in 100 mL of 5 mM of $AgNO_3$ solution using sonication for 30 min. The solution was kept in vacuum for 5cycles. During vacuum cycles most of the silver ions were anchored in the lumen structure as well as silicate cages of HNTs. The silver ion loaded HNTs were collected by whatmnann filtration and then immersed in 1 g green tea in 100 mL aqueous solution for 12 h. spontaneously the solution was changing the color from light pink to dark greenish indicating the formation of Ag-NPs (Fig. 2S). The obtained HNTs/GT/Ag-NPs hybrid material was collected by filtration and dried at 40^oC for 12h. The same amount of GT was added in to the HNTs and designated as HNTs/GT in order to investigate antibacterial performance of GT.

2.3 Characterization of AgNPs

2.3.1 FTIR analysis

A Fourier transform infrared (FTIR) (Perkin Elmer, Wisconsin-410) technique was used to investigate the interactions and structural functional groups of HNTs/GT/Ag-NPs.

2.3.2 Uv-visible measurements

HNT/GT/Ag-NPs dispersion (10mg/10mL Milli-Q water) was prepared for measuring UV-visible spectra using by UV-Visible spectrophotometer (HITACHI U-2010).

2.3.3. XRD analysis

X-ray diffraction (XRD) (Bruker, AXS D8) technique was to investigate the crystalline structure of Ag-NPs presence in HNTs.

2.3.4. SEM-EDS analysis

Scanning electron microscopy (SEM) (JEOL, IT300) and Energy Dispersive Spectroscopy (EDS) (Oxford, X-Max^N) was carried out to investigate the morphology and elemental composition of the HNTs/GT/Ag-NPs respectively

2.3.5. XPS analysis

X-ray Photoelectron Spectroscopy (XPS) (Shimadzu, AXIS Supra™) was to investigate the compositional and quantification of HNTs/GT/Ag-NPs.

2.3.6. TEM analysis

Transmission electron microscopy (TEM) (JEOL, JEM-2010) was used to investigate the morphology and size of Ag-NPs of HNTs/GT/Ag-NPs.

2.3.7. Antibacterial studies

Anti-bacterial activity of HNTs, HNTs/GT and HNTs/GT/Ag-NPs were performed against both gram-negative bacteria Escherichia coli (*E.coli*) (ATCC 25922) and gram-positive Bacillus subtilis (*B.subtilis*) (ATCC6633) using disc diffusion method. 100 μL of bacterial culture were uniformly spread on the solidified nutrient agar medium surface of the petri dishes. The samples (10 mg/10 mL) were loaded with sterilized paper discs and were then placed on the bacterial culture plates. The plates were incubated at 37^oC for 12 h. The inhibition zone was measured around the disc to investigate the effects of bacteria on hybrid materials.

3. Results and Discussion

Green tea (GT) has been shown to have potential antibacterial property against a variety of both gram-positive and gram-negative bacteria [19]. Consequently, in this study, GT mediated reduction of Ag-NPs in the lumen empty space as well as a surface silicate cage of HNTs as a biocompatible nanoclay mineral. Highly biocompatible materials are used for preparing hybrid nanomaterials. Hybrid nanomaterials has been shown environmentally, eco-friendly and enhancing antibacterial property. Antibacterial hybrid nanomaterials are arising and essential materials in the biomedical application. The formation, crystallinity and morphology of Ag-NPs in the HNTs were studied and their antibacterial performance also has been investigated in this work. The schematic representation of preparation of HNT/GT and HNT/GT/Ag-NPs shown in scheme S1.
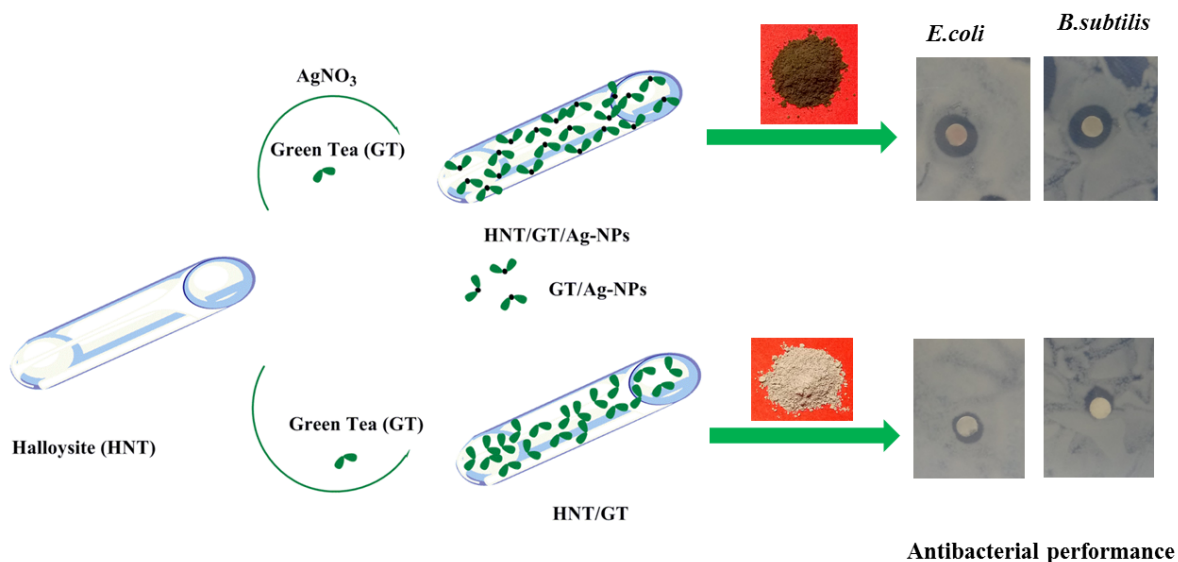
Scheme 1: Schematic representation of preparation of HNT/GT and HNT/GT/Ag-NPs

3.2. *FTIR analysis*

FTIR spectra of HNTs (Fig. 1a) shows two bands at 3619 and 3446 cm^{-1} corresponding to the O−H stretching of inner hydroxyl groups and inner surface hydroxyl groups, respectively. Apical Si−O and Si−O−Si stretching vibrations provided the bands at 1120 and 1007 cm^{-1}, respectively. The bands at 732 and at 678 cm^{-1} are duo to the perpendicular Si−O stretching vibration [17]. After the formation of Ag-NPs in HNTs via GT, the most of the peaks for pristine HNTs remains the same. However, a new peak appeared at 1450 and 1520 cm^{-1} corresponds to GT phenolic −OH and aromatic peaks. The results also show that most of the peaks associated with HNTs shift to lower frequency after formation of Ag-NPs via reduction with GT. These results confirm the presence of GT in the HNTs via hydrogen bonding interaction.

3.3. *Uv-visible Analysis*

The formation of Ag-NPs was investigated by UV-visible spectrophotometry technique. As shown in Fig.1b that there is no peak associated with pristine HNTs. The data, however, show that HNTs/GT/Ag-NPs absorption plasmon peak at 410 nm indicating a successful formation of Ag-NPs.

3.4 XRD analysis

To confirm the crystallinity of Ag-NPs, further the prepared HNTs/GT/Ag-NPs was characterized by XRD technique. As shown in Fig. 1c XRD pattern of pristine HNTs shows 2θ=11°, which corresponds to the basal plane of HNTs. The results show that for HNTs/GT/Ag-NPs, the peaks appear at 38.16°, 44.36°, 64.64°, 77.42° and 81.67° are assigned indexed planes of (111), (200), (220), (311) and (222) respectively. Hence, XRD patterns confirm the face centered cubic structure of Ag-NPs in the HNTs. However, the crystal structure of HNTs is not affected by Ag-NPs.
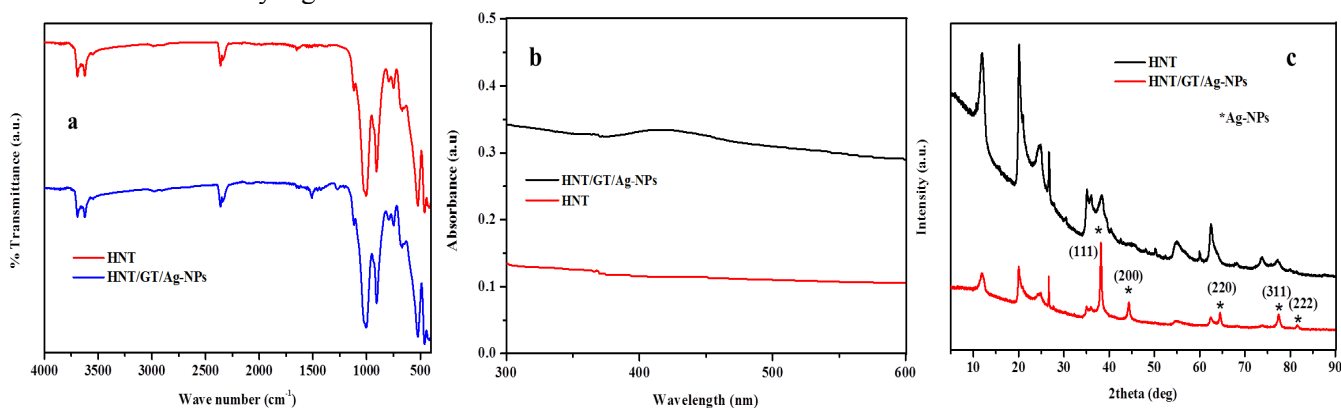

Figure 1: (a) FTIR, (b) UV-Visible spectra and (c) XRD patterns of HNT and HNT/GT/Ag-NPs

3.5. SEM-EDS and TEM analysis

SEM-EDS and XPS techniques were used to further confirm the formation of Ag-NPs in the HNTs. Fig. 2a indicates that HNTs are hollow tube-like structure with smooth surface. Fig. 2b shows rough surface of hollow tubes with aggregation after incorporation with Ag-NPs. The formation of aggregated HNT/GT/Ag-NPs attributed to GT phenolic molecules are entrapped in the HNTs with hydrogen bonding interactions. Fig. 2 (a-1) indicates that the compositional elements O, Si, and Al are observed only in HNTs while fig. 2 (b-1) and fig 3a indicate that O, Si, Al and Ag are observed in the HNTs/GT/Ag-NPs. Fig 3b shows that the Ag 3d region is splitted to form two regions, Ag 3d5/2 and Ag 3d3/2 are assigned to 366.02 and 372.02eV, respectively. These results indicate that stable silver has been produced. Table 1 show that the Ag concentration was evaluated to be 0.43% on the surface of HNTs and 2.1% in HNTs/GT/Ag-NPs. Both techniques complement to each other and confirm the incorporation of Ag-NPs in to the HNTs.

The formation and distribution of Ag-NPs via green tea mediated in the lumen structure as well as surface cage of HNTs were confirmed by TEM image analysis. As shown in Fig. 2c the TEM images of pristine HNTs show empty lumen structure. TEM images of HNT/GT/Ag-NPs (Fig. 2d) show that the highly distributed Ag-NPs were formed in the lumen structure as well as surface cage of HNTs with spherical shape. The spherical shape of Ag-NPs is due to green tea having phenolic hydroxyl groups which were involved the formation of stable spherical Ag-NPs. DLS analysis in fig.S2 shows the size of the extracted Ag-NPs to be average 5 nm
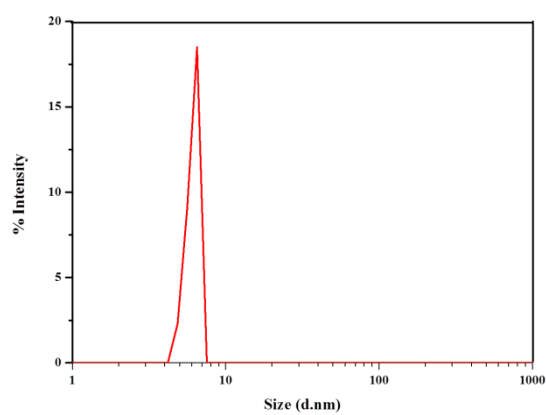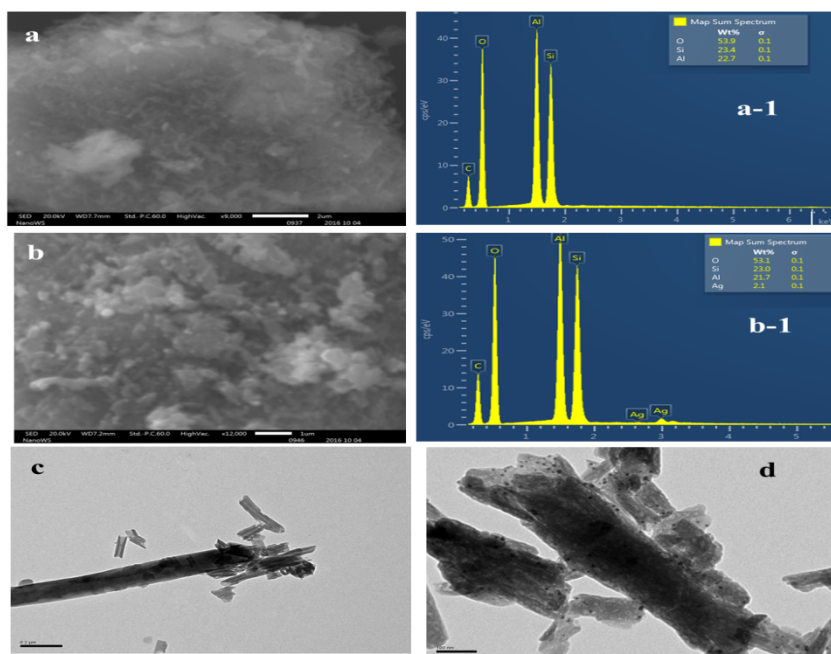

Figure S2: DLS images of Ag-NPs

Figure 2: SEM images of (a) HNT, (b) HNT/GT/Ag-NPs and their EDS spectra of (a-1) HNT and (b-1) HNT/GT/Ag-NPs and TEM images of (c) HNT and (d) HNT/GT/Ag-NPs
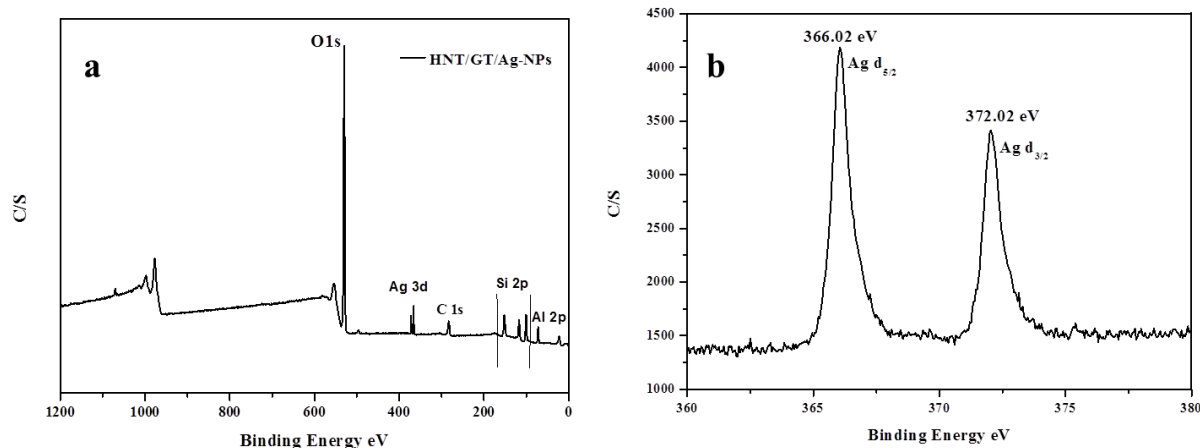
Figure 3: XPS spectra of (a) HNT/GT/Ag-NPs and (b) Ag 3d region

Table 1: SEM-EDS and XPS weight (%) and (%) Surface concentration

Elements	SEM-EDS (Hal/GT/AgNPs)	XPS (Hal/GT/AgNPs)	
	Weight concentration (%)	Mass concentration (%)	Surface concentration (%)
O 1s	53.1	55.66 ± 0.43	69.24 ± 0.38
Si 2p	23.0	22.80 ± 0.44	16.16± 0.34
Al 2p	21.7	19.22 ±0.41	14.18± 0.32
Ag 3d	2.1	2.32±0.15	0.43± 0.03

3.6 *Antibacterial studies*

So far the combination of metallic nanoparticles, antibacterial drugs, and bimetallic nanoparticles has been found to improve the antibacterial activity for many pathogen bacteria [19]. However, in this work GT is used as reducing agent for preparation of Ag-NPs in the lumen and surface silicate cage of HNTs. In addition, GT has great potential as an antimicrobial agent for many pathogens [20]. Hence, the use of GT has more advantageous, not only for reducing Ag^+ ions to its Ag-NPs, but also to enhance the antibacterial activity. Therefore, *E.coli* and Bacillus are bacteria that have been used for antibacterial performance of HNT/GT/Ag-NPs. The disc diffusion method was used for the antibacterial performance as reported elsewhere [21, 22]. Fig. 4 shows that the radial diameters of the inhibition zones for the HNT/GT/Ag-NPs are larger (*E.coli* 16 mm and *B.subtilis* 17.5 mm) than those of HNT/GT, (*E.coli* 8 mm and *B.subtilis* 9 mm), whereas pristine HNT showed no inhibition ability. These result show that the combination of GT with Ag-NPs in the HNTs has potential antibacterial properties and may be suitable for biological applications.
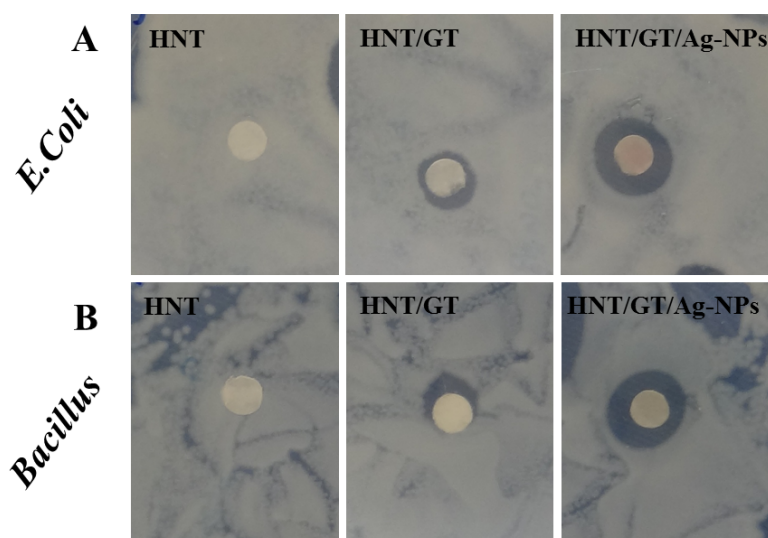

Figure 4: Antibacterial activity of HNT, HNT/GT, and HNT/GT/Ag-NPs on both *E.coli* (a) and (b) *B.subtilis*

Conclusions

In conclusion, a highly uniform spherical shape of Ag-NPs was prepared via green tea mediated reduction in the lumen as well as surface silicate cage of HNTs. The combination of GT and Ag-NPs in HNTs nanohybrid system was effective to antibacterial activity towards both gram-positive and gram-negative bactericides. Hence, the hybrid systems could be administered directly and effectively for antibacterial infections

References

1. K.M.M. Abou El-Nour, A. Eftaiha, A. Al-Warthan, R.A.A. Ammar, *Arabian J. Chem*. 3 (2010) 135.
2. T.K. Sau, C.J. Murphy, *J. Am. Chem. Soc.* 126 (2004) 8648.
3. T. Sakai, P. Alexandridis, *Chem. Mater*. 18 (2006) 2577.
4. Y.S. Shon, E. Cutler, *Langmuir.* 20 (2004) 6626.
5. L. Ge, Q. Li, M. Wang, J. Ouyang, X Li, M.M. Xing, *Inter. J. Nanomed.* 9 (2014) 2399.
6. P. Sanpui, A. Murugadoss, P.V.D. Prasad., S.S. Ghosh., A. Chattopadhyay, *Int. J. Food Microbiol.* 124 (2008) 142.
7. J. Fu, J. Ji, D. Fan, J. Shen, *J. Biomed. Mater Res. Part A.* 79 (2006) 665.
8. D. Xiaoxu, W. Huixian, C. Weihang, L. Jindun, Z. Yatao, *RSC Adv*. 44 (2014)1993.
9. Z. Shuting., F. Rouowen, W. Dingcai, X. Wei Y. Qiwei, C. Zhangliu, *Carbon.* 42 (2004) 3209.
10. A. Murugadoss, A. Chattopadhyay, *Nanotech.* 19 (2008) 015603.
11. L. Jibin, H. Yu Sik, J. Lenhart, J. *Environ. Sci. Nano.* 2 (2015) 528.
12. E. Joussein, S. Petit, J. Churchman, B. Theng, D. Righi, B. Delvaux, *Clay Minerals.* 40 (2005) 383.
13. V. Vergaro, E. Abdullayev, Y.M. Lvov, A. Zeitoun, R. Cingolani ,R. Rinaldi, S. Leporatti, *Biomacromol.* 11 (2010) 820.
14. J. Tully, Y. Raghuvara, Y. Lvov, *Biomacromol.* 17 (2016) 615.
15. Y.M. Lvov, D.G. Shchukin, H. Mohwald, R.R. Price, *ACS Nano.* 2 (2008) 814.
16. Y. Lvov, W. Wang, L. Zhang, R. Fakhrullin, *Adv. Mater.* 28 (2016)1227.
17. Y. Zhang, Y. Chen, H. Zhang, B. Zhang, J. Liu, *J. Inorg. Biochem.* 118 (2013) 59.
18. E. Abdullayev, K. Sakakibara, K. Okamoto, W. Wei, K. Ariga, Y. Lvov, *ACS Appl. Mat & Interfac.* 3 (2011) 4040.
19. K. Varaprasad, G. Siva Mohan Reddy, J. Jayaramudu, R. Sadiku, K. Ramam, S. Sinha Ray, *Biomater. Sci.* 2 (2014) 257.
20. C. Reygaert Wanda, *Front. in Microbiol*. 5 (2014) 434.
21. S. Ravindra, K. Varaprasad, V. Rajinikanth, A.F. Mulaba-Bafubiandi, K.V.S. Ramam, *J. Macromol. Sci. Part A*. 12 (2013) 1230.
22. E. Chandra Sekhar, K.S.V. Krishna Rao, K. Madhusudhana Rao, *Mater. Lett.* 174 (2016) 129.

(2018) ; http://www.jmaterenvironsci.com